

# On the structure and optical band gap in $(\text{Bi}_2\text{O}_3)_{0.2}(\text{BaO})_x(\text{B}_2\text{O}_3)_{0.8-2x}(\text{GeO}_2)_x$ glasses

H. TICHÁ, J. SCHWARZ, L. TICHÝ<sup>a,b\*</sup>

*Faculty of Chemical Technology, University of Pardubice, 532 10 Pardubice, Czech Republic*

<sup>a</sup>*Institute of Macromolecular Chemistry of the Academy of Sciences of the Czech Republic v.v.i., Heyrovsky sq. 2, 120 06 Prague, Czech Republic*

<sup>b</sup>*Joint Laboratory of Solid State Chemistry of University of Pardubice and Institute of Macromolecular Chemistry of the Academy of Sciences of the Czech Republic v.v.i., Studentska 84, 532 10 Pardubice, Czech Republic*

New  $(\text{Bi}_2\text{O}_3)_{0.2}(\text{BaO})_x(\text{B}_2\text{O}_3)_{0.8-2x}(\text{GeO}_2)_x$  glasses were prepared from pure oxides. The glass transition temperatures decreased from 489 to 460 °C with the increase in  $x$  from 0.05 to 0.3, simultaneously the coefficient of thermal expansion increased from 7.3 to 9.6 ppm °C<sup>-1</sup>. The optical band gap was determined in the region 3.84 ( $x = 0.05$ ) – 3.54 eV for  $x = 0.3$ , the coefficient of the temperature dependence of the optical gap for the temperatures between 30 and 250 °C was found in the narrow region  $3.3 \times 10^{-4} - 4 \times 10^{-4}$  eV K<sup>-1</sup> and the non-linear refractive index of the studied glasses was estimated from the optical gap values at around  $6.9 \times 10^{-11}$  esu. Possible structural arrangement of the glasses prepared as indicated by Raman spectroscopy was discussed.

(Received May 30, 2013; accepted September 18, 2013)

*Keywords:* Oxide glasses, Raman spectroscopy, optical properties

## 1. Introduction

In recent years preparation and physical properties of various quaternary glasses based on heavy metal oxides (HMO) namely on  $\text{Bi}_2\text{O}_3$  have been studied. Nitta et al. [1] reported glass forming regions in  $\text{Bi}_2\text{O}_3$ -ZnO-10 $\text{B}_2\text{O}_3$ - $\text{R}_2\text{O}$  ( $\text{R} = \text{Li}, \text{Na}, \text{K}$ ) systems and the values of the glass-transition temperature for the glasses studied. Dyamant et al. [2] described the glass-formation region in  $\text{SiO}_2$ - $\text{B}_2\text{O}_3$ - $\text{Bi}_2\text{O}_3$ -ZnO and determined the glass-transition temperatures, the dilatometric softening points and the coefficient of thermal expansion for various glasses studied. Kassab et al. [3] found that  $\text{PbO}$ - $\text{Bi}_2\text{O}_3$ - $\text{Ga}_2\text{O}_3$ -BaO glass doped by  $\text{Nd}_2\text{O}_3$  is a good candidate for photonic devices active in the infrared spectral region. Bale et al. [4] found that for  $(\text{Bi}_2\text{O}_3)_{0.75-x}(\text{Li}_2\text{O})_x(\text{ZnO})_{0.1}(\text{B}_2\text{O}_3)_{0.15}$  glasses an increase in  $\text{Bi}_2\text{O}_3$  content leads to conversion of three-fold to four-fold coordinated boron. Knoblochova et al. [5] determined the optical band gap, the coefficient of the temperature dependence of the optical band gap and also estimated the non-linear refractive index in  $(\text{Bi}_2\text{O}_3)_{0.2}(\text{PbO})_x(\text{B}_2\text{O}_3)_{0.82x}(\text{GeO}_2)_x$  glasses.

Srinivasu et al. [6] studied structural and transport properties of certain  $\text{LiF}$ - $\text{Li}_2\text{O}$ - $\text{SrO}$ - $\text{Bi}_2\text{O}_3$  glasses and found a decrease in the glass-transition temperature with an increase in the content of  $\text{LiF}$ , simultaneously due to a mixed contribution of  $\text{Li}^+$  and  $\text{F}^-$  ions and an increase in the dc electrical conductivity was claimed.

In order to extend the family of quaternary glasses based on  $\text{Bi}_2\text{O}_3$  the presented work is focused on  $(\text{Bi}_2\text{O}_3)_{0.2}(\text{BaO})_x(\text{B}_2\text{O}_3)_{0.8-2x}(\text{GeO}_2)_x$  glasses, the BaO

analog to the glasses we reported previously [5]. We examined the possible structural arrangement of the glassy network as inferred from Raman spectroscopy and we determined the optical band gap for  $(\text{Bi}_2\text{O}_3)_{0.2}(\text{BaO})_x(\text{B}_2\text{O}_3)_{0.8-2x}(\text{GeO}_2)_x$  glasses where  $0.05 \leq x \leq 0.3$ .

## 2. Experimental details

Glasses with the chemical composition  $(\text{Bi}_2\text{O}_3)_{0.2}(\text{BaO})_x(\text{B}_2\text{O}_3)_{0.8-2x}(\text{GeO}_2)_x$  ( $x = 0.05, 0.1, 0.15, 0.2, 0.3$ ), see Table 1, were prepared using a conventional melt-quenching method. High purity (4N)  $\text{Bi}_2\text{O}_3$ ,  $\text{GeO}_2$ ,  $\text{H}_3\text{BO}_3$  and  $\text{Ba}(\text{NO}_3)_2$  for 20 g batches were mixed together and melted in a covered corundum crucible at the temperatures  $T = 810 - 890$  °C (according to their chemical composition) in a preheated electric furnace. After 20 minutes of melting and homogenization, the melts were poured onto a nickel plate heated to 150 °C, covered by a heat insulating cover and slowly cooled down for 60 minutes to the ambient temperature. Compact, clear, transparent glasses with a weak yellowish tint were obtained. The chemical composition of the prepared glasses was verified using a microprobe X-ray analysis (JEOL JSM 5500 LV). Special attention was paid to the determination of the content of the aluminium which varied in the region 0.7 – 1.2 at%.

The hydrostatic density ( $\rho$ ) of the bulk samples (a sample mass around 3g) was determined at room temperature in distilled water. From five replicated measurements the density values were accurate within

$\pm 1\%$ . The calculated molar volume values,  $V_m (= M/\rho, M$  is the average molar weight) were accurate within  $0.05 \text{ cm}^3/\text{mol}$ .

The values of the glass-transition temperature ( $T_g$ ) and the coefficient of the thermal expansion (CTE) of the glasses prepared were determined employing a thermo mechanical analysis. The samples (approximately  $5 \times 5 \times 5 \text{ mm}$ ) were heated from an ambient temperature up to the deformation temperature of the glass in a TMA CX04 thermo-mechanical analyzer at a heating rate of  $5 \text{ K/min}$ , load  $\approx 10 \text{ mN}$ . From the “low” temperature and “high” temperature expansion curves of the glass the glass-transition temperature ( $T_g$ ) was determined using the slope intercept method and the coefficient of the thermal expansion ( $\alpha$ ) was determined from the “low” temperature expansion “curve” in the temperature region  $100 - 300 \text{ }^\circ\text{C}$ .

Optical investigations were performed by transmission (T) measurements in the UV-VIS spectral region employing an optical thermostat O.T.I. (R.M.I.) placed in the sample compartment of HP 8453 spectrophotometer in the temperature region of from  $300$  to approximately  $600 \text{ K}$ . The samples prepared by glass blowing were used with a thickness (d) at around  $2 - 4 \text{ }\mu\text{m}$ ; their chemical composition was verified using a microprobe X-ray analysis (JEOL JSM 5500 LV) with a precision  $\pm 1.5\%$  in the atomic fraction of the elements. Optical band gap values ( $E_g$ ) were determined from Tauc plots [7]:  $(K\text{h}\nu)^{1/2} = B^{1/2}(\text{h}\nu - E_g)$ , where  $B^{1/2}$  is the slope of the short wavelength absorption edge (SWAE),  $\text{h}\nu$  is the photon energy,  $K$  is the absorption coefficient, and the power exponent  $1/2$  reflects the non-direct type of optical transition between the valence and conduction band. The values of the absorption coefficient were calculated using the relation  $K = (1/d) \ln\{[(1-R)^2 + ((1-R)^4 + 4R^2T^2)^{1/2}]/2T\}$  [8], where  $R$  is the reflectance, respectively. The values of  $R \approx 0.11$  invariant to the wavelength within a narrow spectral region of SWAE, were used to determine  $K$  values.

The Raman spectra were recorded using the Fourier transform infrared (FTIR) spectrometer Bruker model IFS 55 equipped with the FRA 106 Raman module in back scattering geometry using a Nd:YAG laser beam (excitation light wavelength  $\lambda = 1064 \text{ nm}$ , slit width  $4 \text{ cm}^{-1}$ , laser power  $\approx 300 \text{ mW}$  at the sample surface). All spectra were measured at ambient temperature in the spectral region  $50\text{--}1500 \text{ cm}^{-1}$  using 200 scans on the bulk sample with a flat optically polished surface. The intensity of experimental spectra ( $I_{\text{exp}}$ ) were reduced ( $I_{\text{red}}$ ) using the Bose-Einstein population factor,  $I_{\text{red}}(\nu) = I_{\text{exp}}(\nu)[n(\nu, T) + 1]^{-1}$ ,  $n(\nu, T) = [\exp(\text{h}\nu/k_B T) - 1]^{-1}$ , where  $\nu$ ,  $k_B$  and  $T$  represent the observed Raman shift, Boltzmann constant and the temperature,  $T = 300 \text{ K}$ , respectively. In this case and with respect to the fact that our glasses are, neglecting the Fresnel reflection, transparent for the Nd:YAG laser beam and hence the penetration depth of the excitation light significantly exceeds the sample thickness, we used Raman intensities of certain Raman features for the semi quantitative comparison.

### 3. Results

#### 3.1 Certain characteristics of $(\text{Bi}_2\text{O}_3)_{0.2}(\text{BaO})_x(\text{B}_2\text{O}_3)_{0.8-2x}(\text{GeO}_2)_x$ glasses

The chemical composition of the glasses studied and the values of the hydrostatic density, the molar volume, the glass-transition temperature and the coefficient of the thermal expansion are summarized in Table 1. For comparison the values of certain relevant quantities for  $(\text{Bi}_2\text{O}_3)_{0.2}(\text{PbO})_x(\text{B}_2\text{O}_3)_{0.8-2x}(\text{GeO}_2)_x$  glasses are quoted in the parenthesis [5]. As expected, the formal substitution of  $\text{PbO}$  by  $\text{BaO}$  resulted in a decrease in the density due to  $\rho(\text{PbO}) \approx 9.53 \text{ g/cm}^3$  and  $\rho(\text{BaO}) \approx 5.72 \text{ g/cm}^3$ .

Table 1 The chemical composition expressed as the ratio of the molar fraction of substituents ( $x$ ) to the molar fraction of  $\text{B}_2\text{O}_3$ , the density ( $\rho$ ), the molar volume ( $V_m$ ), the dilatometric glass transition temperature ( $T_g$ ), the coefficient of thermal expansion (CTE) and the optical band gap ( $E_{g, \text{non}}$ ) of  $(\text{Bi}_2\text{O}_3)_{0.2}(\text{BaO})_x(\text{B}_2\text{O}_3)_{0.8-2x}(\text{GeO}_2)_x$  glasses. The corresponding values for  $(\text{Bi}_2\text{O}_3)_{0.2}(\text{PbO})_x(\text{B}_2\text{O}_3)_{0.8-2x}(\text{GeO}_2)_x$  glasses are shown in the parenthesis [5].

$x/\text{B}_2\text{O}_3$	$\rho$ [ $\text{g/cm}^3$ ]	$V_m$ [ $\text{cm}^3/\text{mol}$ ]	$T_g$ [ $^\circ\text{C}$ ]	CTE [ppm/ $^\circ\text{C}$ ]	$E_{g, \text{non}}$ [eV]
0.05/0.7	4.48 (5.85)	34.56 (27.06)	489 (448)	7.3	3.84 (3.6)
0.1/0.6	4.92 (6.01)	32.68 (27.91)	474 (425)	8.2	3.75 (3.57)
0.15/0.5	5.2	31.10	470	8.5	3.72
0.2/0.4	5.59 (6.64)	30.88 (28.11)	466 (400)	9.0	3.68 (3.53)
0.3/0.2	5.99 (7.02)	30.8 (29.25)	460 (385)	9.6	3.54 (3.46)

The relative error in the density values does not exceed  $\pm 1\%$ , the error in  $T_g$  is estimated  $\pm 2 \text{ }^\circ\text{C}$ , the error in CTE values is estimated  $\pm 0.75 \text{ ppm}/^\circ\text{C}$  and the relative error in  $E_g$  is less than  $5\%$ .

The values of the molar volume are higher for  $\text{BaO}$  glasses which is consistent with the higher molar volume of  $\text{BaO}$  ( $V_M \approx 26.8 \text{ cm}^3/\text{mol}$ ) in comparison with  $V_M(\text{PbO}) \approx 23.5 \text{ cm}^3/\text{mol}$ . The glass transition decreases with a decrease in the content of  $\text{B}_2\text{O}_3$  (and with an increase in

$\text{BaO}/\text{GeO}_2$  content, which indicates a decrease in both the overall cohesive forces and the connectedness of the network. However, the  $T_g$  values for  $\text{BaO}$  glasses are higher than the  $T_g$  values for the corresponding  $\text{PbO}$  glasses ( $x(\text{PbO}) = x(\text{BaO})$ ). The reason could be that even

if both PbO and BaO behave as modifiers, the strength of the Pb-O bond equals  $\approx 99$  kcal/mol, the strength of the BaO bond equals  $\approx 116$  kcal/mol [9] and therefore the overall cohesive forces could be higher in the glasses where PbO is substituted by BaO. As expected, the CTE values increased with a decrease in the glass-transition temperature, Table 1. In Fig. 1 typical spectral dependences of  $(Kh\nu)^{1/2}$  versus  $h\nu$  ( $x = 0.1$ ), the sample thickness was  $d = 2.75 \mu\text{m}$ , are shown. The values of the non-direct optical band gap ( $E_g = h\nu(K \rightarrow 0)$ ) are displayed in Table 1.

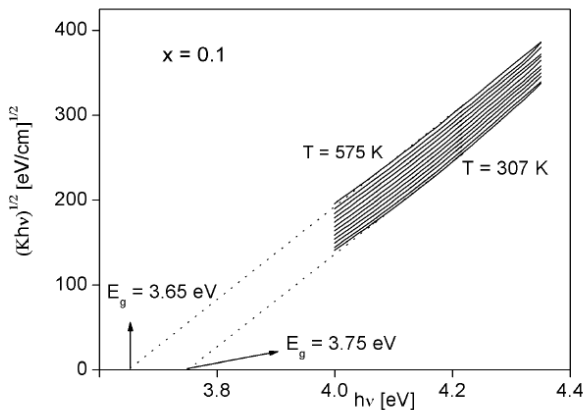


Fig. 1. Illustration of the typical red shift of the absorption edge in the coordinates  $(Kh\nu)^{1/2}$  vs.  $h\nu$ , for  $(\text{Bi}_2\text{O}_3)_{0.2}(\text{BaO})_{0.1}(\text{B}_2\text{O}_3)_{0.6}(\text{GeO}_2)_{0.1}$  glass, the thickness  $d = 1.74 \mu\text{m}$ . The temperature increment is about 25-28 °C. The dashed line illustrates the way of the optical band gap determination.

The temperature dependences of the optical band gap shown in Fig. 2 follow the simple relation:  $E_g(T) = E_g(0) - \gamma T$ . The values of  $\gamma \approx 3.5 \times 10^{-4} \text{ eVK}^{-1}$  are nearly independent on the chemical composition.

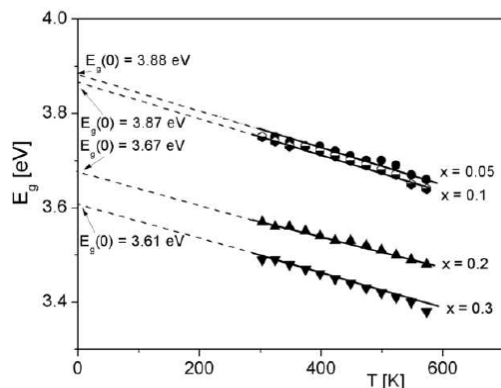


Fig. 2 The temperature dependence of the optical band gap for  $(\text{Bi}_2\text{O}_3)_{0.2}(\text{BaO})_x(\text{B}_2\text{O}_3)_{0.8-2x}(\text{GeO}_2)_x$  glasses. Dashed lines illustrate the linear extrapolation according to relation:  $E_{g,non}(T) = E_{g,non}(0) - \gamma T$ .

It is obvious from Table 1 that the optical band gap decreases with an increase in the BaO content, however, for the corresponding glasses it is valid that  $E_g(\text{BaO}) > E_g(\text{PbO})$ .

### 3.2. Raman spectra

The corrected Raman spectra for glasses where  $x = 0.05, 0.1, 0.2, 0.3$  are displayed in Fig. 3.

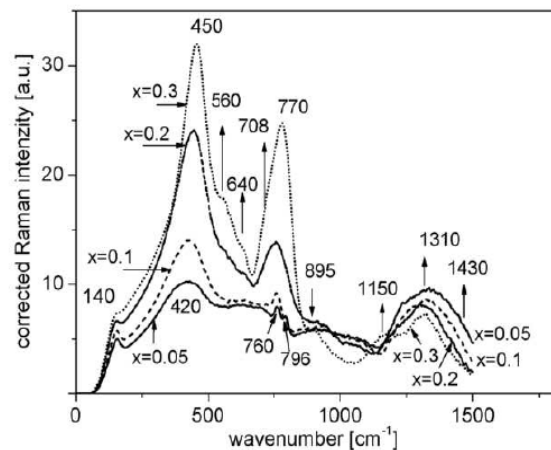


Fig. 3 The corrected Raman spectra of  $(\text{Bi}_2\text{O}_3)_{0.2}(\text{BaO})_x(\text{B}_2\text{O}_3)_{0.8-2x}(\text{GeO}_2)_x$  glasses. The numbers above the spectra mark the wavenumber of maxima of relevant Raman band. The numbers on the left hand side indicate the chemical composition ( $x$ ).

For simplicity the observed RF were divided into two basic parts:

(i) RF associated with vibrations of boron-oxygen structural units. As is widely accepted, for instance [10] and the cited references [10,13-15], the Raman activity of  $[\text{BO}_4]^{5-}$  tetrahedron corresponds to the four normal vibrations with the wavenumbers:  $\delta \sim 600 \text{ cm}^{-1}$ ,  $\gamma \sim 400-600 \text{ cm}^{-1}$ ,  $\nu_s \sim 740-890 \text{ cm}^{-1}$ ,  $\nu_{as} \sim 1000-1150 \text{ cm}^{-1}$  and the Raman activity of the  $[\text{BO}_3]^{3-}$  groups corresponds to the following normal vibrations with the wavenumbers:  $\delta \sim 500-600 \text{ cm}^{-1}$ ,  $\gamma \sim 650-800 \text{ cm}^{-1}$ ,  $\nu_s \sim 850-960 \text{ cm}^{-1}$ ,  $\nu_{as} \sim 1100-1450 \text{ cm}^{-1}$ . Here  $\delta$ ,  $\gamma$  and  $\nu$  belong to in plane bending, out of plane bending and stretching vibrations, respectively. We suppose that the RF we observed in the high wavenumber region ( $1000 < \nu < 1500 \text{ cm}^{-1}$ ), Fig. 3, suggests that namely in the glasses where  $x < 0.3$  the borate network is in all probability primarily formed by  $[\text{BO}_3]^{3-}$  groups.

(ii) RF associated with a response related to the presence of heavy metal oxides [11-13]: (a)  $\text{RF}_{\text{HM}}$  due to a motion of heavy metal ions,  $\nu \sim 70 - 160 \text{ cm}^{-1}$ .  $\text{RF}_{\text{AC}}$  due to acoustic phonons, the wavenumber region  $\nu \sim 50 - 100 \text{ cm}^{-1}$  we did not observe owing to our experimental arrangement. (b)  $\text{RF}_{\text{BA}}$  due to “bridged-anion” (symmetric stretch motion of an anion (A) in C-A-C bridge, here C is a cation),  $\nu \sim 360 - 600 \text{ cm}^{-1}$ , and (c)  $\text{RF}_{\text{NBA}}$ , the wavenumber region  $\nu \sim 650 - 950 \text{ cm}^{-1}$  due to “non-bridged-anion” which is an asymmetric C’ – A-C bridge (the bond length of C’ – A bond is longer than that of C-A

bond). For the usual case: A = oxygen the origin of  $\text{RF}_{\text{NBA}}$  could also be the C-O configuration [13]. Fig. 3 indicates that with an increase in  $x$  the RF at around  $420\text{-}450\text{ cm}^{-1}$  ( $\text{RF}_{(420-450)}$ ) and the RF at around  $760\text{-}770\text{ cm}^{-1}$  ( $\text{RF}_{(760-770)}$ ) become well developed. The ratio ( $r$ ) of intensities ( $I$ ) of  $\text{RF}_{(1310)}/\text{RF}_{(770)}$  and  $\text{RF}_{(1310)}/\text{RF}_{(420-450)}$  monotonically decreases with an increase in  $x$ , while for  $r = I(\text{RF}_{(770)})/I(\text{RF}_{(420-450)})$  a decrease from  $r(x=0.05) = 0.77$  to  $r(x=0.2) = 0.57$  was observed and for  $x = 0.3$  the value  $r(x=0.3) = 0.8$  was obtained. We are of the opinion that: (a) a monotonous decrease in  $r_{(1310/770)}$  and  $r_{(1310/420-450)}$  reflects in particular the changes in the chemical composition of the glasses studied, that is a decrease in the content of  $\text{B}_2\text{O}_3$  and an increase in the influence of HMO in the Raman response and (b) the non-monotonous dependence of  $r_{(770/420-450)}$  on the chemical composition together with relatively well developed  $\text{RF}_{(420-450)}$  and  $\text{RF}_{(760-770)}$  indicates certain structural changes associated, namely for  $x = 0.2$  and  $0.3$ , with an ordering.

## 4. Discussion

### 4.1. Some structural considerations inferred from Raman spectra

#### 4.1.1 Wavenumber region $1000\text{ cm}^{-1} < \nu < 1500\text{ cm}^{-1}$

We assign the broad RF in the wavenumber region  $1000 - 1500\text{ cm}^{-1}$  particularly to Raman activity of  $\text{BO}_3$  group see, for instance [10]. Specifically this broad RF can be attributed to an overlap of the following modes: (i) B-O<sup>-</sup> in  $\text{BO}_2\text{O}^-$ , (ii)  $\text{BO}_2\text{O}^-$  triangle linked to  $\text{BO}_4$  unit [14] and (iii) stretching in  $\text{BO}_3$  triangles which are, however, asymmetrically connected [15]. For  $x = 0.2$  and  $0.3$  the broad  $\text{RF}_{(1000-1500)}$  is separated into at least two RF with the maximum at around  $1150\text{ cm}^{-1}$  ( $\text{RF}_{(1150)}$ ) and at around  $1310\text{ cm}^{-1}$  ( $\text{RF}_{(1310)}$ ), respectively.  $\text{RF}_{(1150)}$  indicates that the broadening of  $\text{RF}_{(1000-1500)}$  into the lower wavenumber region reflects the presence of  $\text{BO}_4$  structural units since  $\text{RF}_{(1150)}$  may be attributed to  $\nu_{\text{as}}$  ( $\approx 1000\text{-}1150\text{ cm}^{-1}$ ) of  $[\text{BO}_4]^{2-}$  tetrahedron [10]. This suggestion is in harmony with the fact that BaO known as a typical modifier assists not only in the formation of non-bridging sites such as Ba-O-B but also converts  $\text{BO}_3$  to  $\text{BO}_4$  units [16, 17].

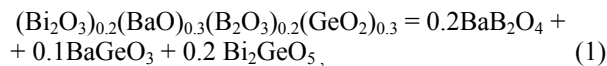
#### 4.1.2 Wavenumber region $100\text{ cm}^{-1} < \nu < 1000\text{ cm}^{-1}$

We focused specifically on the three well resolved Raman features at around  $140\text{ cm}^{-1}$  ( $\text{RF}_{(140)}$ ),  $420 - 450\text{ cm}^{-1}$  ( $\text{RF}_{(420-450)}$ ), and  $760 - 770\text{ cm}^{-1}$  ( $\text{RF}_{(760-770)}$ ). Within the classification of Raman activity of HMO glasses by Lines [11, 12] and Miller et al. [13] these RF can be attributed as follows: (a)  $\text{RF}_{(140)}$  to vibrational modes due to  $\text{Bi}^{3+}$  motion. A seemingly surprising increase in the intensity of this RF for the constant molar content of  $\text{Bi}_2\text{O}_3$  (20%) may be assigned (even for the case of constant Raman activity of this RF) to the fact that with an increase in  $x$  the formal volume fraction of  $\text{Bi}_2\text{O}_3$  also

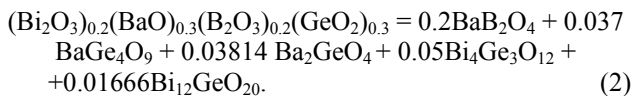
increases from 25.9 vol.% ( $x = 0.05$ ) to 29.7 vol.% ( $x = 0.3$ ). (b)  $\text{RF}_{(420-450)}$  to “bridged-anion” motion ( $\text{RF}_{\text{BA}}$ ) due to a symmetric stretch motion of oxygen in the Bi-O-Bi bridge which, however, could be combined with Bi-O-Ge “non-bridged-anion” motion ( $\text{RF}_{\text{NBA}}$ ) and/or with non-bridging oxygen motion in Bi-O<sup>-</sup> of the  $\text{BiO}_6$  octahedral unit, for instance, the “knee” type RF at around  $620\text{ cm}^{-1}$  ( $\text{RF}_{(620)}$ ) seen for  $x = 0.2, 0.3$ . However, a significant increase in the Raman intensity of  $I(\text{RF}_{(420-450)})$  with an increase in the formal content of  $\text{GeO}_2$  implies that RF due to oxygen motion in Ge-O-Ge linkage ( $\nu \approx 420 - 450\text{ cm}^{-1}$ ) also contributes to  $I(\text{RF}_{(420-450)})$  [18, 19]. (c) With an increase in  $\text{GeO}_2$  content the intensity of  $\text{RF}_{(760-770)}$  increases which indicates the presence of non-bridged-oxygen (NBO) units with Ge-O<sup>-</sup> configuration because  $\text{RF}_{(760-770)}$  corresponds to symmetric stretching vibrations of Ge-O<sup>-</sup> bonds [20], or in other words it indicates the presence of  $\text{GeO}_4$  tetrahedra with two NBO. The shoulder of  $\text{RF}_{(760-770)}$  seen at around  $708\text{ cm}^{-1}$  is attributed to asymmetric stretching Ge-O<sup>-</sup> vibration in  $\text{GeO}_4$  units having four NBOs [20]. For both  $\text{RF}_{(420-450)}$  and  $\text{RF}_{(760-770)}$  a linear correlation between both  $I(\text{RF}_{(420-450)})$  and  $I(\text{RF}_{(760-770)})$  and the formal volume fraction ( $y$ ) of  $\text{GeO}_2$  exists with  $R_{\text{sq}} = 0.99$  for  $I(\text{RF}_{(420-450)}) = 6.69 + 1.06 \times y$  and with  $R_{\text{sq}} = 0.95$  for  $I(\text{RF}_{(760-770)}) = 3.74 + 0.8 \times y$ , ( $y$  in vol %). Despite the correlation between  $I(\text{RF}_{(420-450)})$  and  $y$ , we suppose that this feature and its broadening into the low wavenumber region also reflects the presence of ( $\text{RF}_{\text{BA}}$ ) due to the symmetric stretch motion of oxygen in Bi-O-Bi bridge [11-13].

Of interest is the fact that Raman spectra of  $(\text{Bi}_2\text{O}_3)_{0.2}(\text{BaO})_x(\text{B}_2\text{O}_3)_{0.8-2x}(\text{GeO}_2)_x$  glasses namely for  $x \geq 0.2$ , the wavenumber region  $250 - 1000\text{ cm}^{-1}$  are well structured with two dominant RF at around  $450$  and  $770\text{ cm}^{-1}$ . We speculate that a possible reason for such well developed Raman spectra could be the formation of certain compounds of which some structural units assist in the ordering of a glass network. Following Markova et al. [21] we assume that an increase in  $I(\text{RF}_{(760-770)})$ , namely for  $x = 0.2$  and  $0.3$ , may be attributed to the formation of structural entities inherent to  $\text{BaB}_2\text{O}_4$ ,  $\text{BaB}_4\text{O}_7$ , or  $\text{BaB}_8\text{O}_{13}$  (BBO) compounds. We note that barium borate is formed even during the mixing of BaO and  $\text{B}_2\text{O}_3$  at room temperature [22]. Hence we assume that BBO compounds can participate in the network formation of BBBGO glasses. The other BaO based compounds which can assist in BBBGO glasses network formation could be  $\text{BaGeO}_3$ ,  $\text{BaGe}_4\text{O}_9$ ,  $\text{Ba}_2\text{GeO}_4$  or  $\text{Ba}_3\text{GeO}_5$  [23] namely those B-Ge-O compounds having well pronounced structural make-up based mainly on layers and chains of  $\text{GeO}_4$  tetrahedra that is the structural arrangement which generally assists in the glass-formation. Unfortunately, only the Raman spectra for  $\text{BaGe}_4\text{O}_9$  were found of which the most intensive RF is however at around  $550\text{ cm}^{-1}$  [24] the wave number region where we observed only a knee on the higher wave number side of  $\text{RF}_{(420-450)}$  but it is not consistent with observed strong  $\text{RF}_{(420-450)}$ , see Fig. 3. The other possible compound of which structural units may assist the BBBGO glasses formation could be  $\text{BaGeO}_3$  having a structural make-up based just on layers and chains of

GeO<sub>4</sub> tetrahedra [25]. Based on the dissimilarity of Raman spectra we, in the first approximation, excluded from consideration the series of Bi-B-O compounds which are formed in the Bi<sub>2</sub>O<sub>3</sub> - B<sub>2</sub>O<sub>3</sub> system [10] and also the structural units inherent to BaBiBO<sub>4</sub> [26]. However, the other possible compounds based on Bi<sub>2</sub>O<sub>3</sub> (for instance Bi<sub>2</sub>GeO<sub>5</sub>, Bi<sub>2</sub>Ge<sub>3</sub>O<sub>9</sub>, Bi<sub>4</sub>Ge<sub>3</sub>O<sub>12</sub> and Bi<sub>12</sub>GeO<sub>20</sub> [27]) could assist in the network formation. Out of these compounds except of Bi<sub>12</sub>GeO<sub>20</sub> of which main RF were observed at around 150, 260, 310 and 535 cm<sup>-1</sup>, respectively [28], only Raman spectrum of crystalline and glassy Bi<sub>4</sub>Ge<sub>3</sub>O<sub>12</sub> with the most intensive RF at around 400 cm<sup>-1</sup> for the glassy state is known to us [29]. Hence it is not possible to unambiguously suggest which Bi-Ge-O compound could primarily participate in the overall structural make-up of BBBGO glasses. However, owing to well structured Raman spectra we would assume that in BBBGO glasses the structural make-up could be to some extent ordered, hence certain quite stable structural units must be formed there. Consequently, for instance the glass with x = 0.3, one can ad hoc express in the simple (1) or little bit more complicated form (2):



or



Further work is necessary to identify precisely the compounds of which structural units assist to the structural make-up of BBBGO glasses

#### 4.2 The optical energy gap and its temperature dependence

From Table 1 it is apparent that the differences in the optical band gap values between BBBGO and BPBGO glasses are relatively small and decrease from 6.25% for x = 0.05 to 2.26% for x = 0.3, the optical energy gap decreases with a decrease in the content of B<sub>2</sub>O<sub>3</sub> and with an increase in the content of GeO<sub>2</sub> and BaO. We are of the opinion that the optical band gap narrowing with an increase in x and quite small differences in the E<sub>g</sub> of BBBGO and BPBGO glasses is a consequence of the similar origin of the top of the valence band. In both glasses Raman spectra indicate the presence of the non-bridging oxygen atoms namely as a result of the creation of B<sub>2</sub>O<sup>-</sup> triangles, Bi-O<sup>-</sup> and Ge-O<sup>-</sup> configurations. The states based on the non-bridging oxygen form the top of the valence band, are more susceptible to excitation than the states based on the bridging oxygen and hence the optical band gap is reduced with an increase in the density of states based on NBO. The values of the coefficient of the temperature dependences of the optical band gap are only slightly changing with an increase in x. Taking  $\gamma = Ak_B/\hbar\omega_E$  [30] where, A is the sum of an intrinsic constant volume contribution and thermal expansion,

respectively [31] and  $\hbar\omega_E$  is the energy of the Einstein oscillator we suppose that, since the CTE values only little bit increases with substitution of B<sub>2</sub>O<sub>3</sub> by BaO and GeO<sub>2</sub> most probably  $\hbar\omega_E$  remains to be nearly constant and hence only negligible changes in  $\gamma$  were observed. Lastly, following the simple empirical relation  $n_2[\text{esu}] \approx 1.26 \times 10^{-9}/(E_g)^4$  [32] we estimated n<sub>2</sub> values in the region  $5.8 \times 10^{12} \text{ esu} < n_2 < 8. \times 10^{12} \text{ esu}$  which are comparable to  $n_2 \approx 8.15 \times 10^{-12} \text{ esu}$  estimated for BPBGO glasses [5].

## 5. Conclusion

Our results can be summarized as follows:

(i) New (Bi<sub>2</sub>O<sub>3</sub>)<sub>0.2</sub>(BaO)<sub>x</sub>(B<sub>2</sub>O<sub>3</sub>)<sub>0.8-2x</sub>(GeO<sub>2</sub>)<sub>x</sub> glasses were prepared.

(ii) Both the glass transition temperature (T<sub>g</sub>) and the non-direct optical band (E<sub>g,non</sub>) decreased with a decrease in B<sub>2</sub>O<sub>3</sub> content and with an increase in BaO and GeO<sub>2</sub> content.

(iii) Raman spectra indicated that with an increase in BaO and GeO<sub>2</sub> content the density of units with the non-bridging oxygen increased hence the network connectivity and overall cohesive forces decreased which corresponded with a decrease in both T<sub>g</sub> and E<sub>g,non</sub>.

## Acknowledgement

Support from the Faculty of Chemical Technology, University of Pardubice is acknowledged by H. Ticha and J. Schwarz, institutional support RVO: 61389013 is acknowledged by L. Tichy. We are indebted to prof. M. Vlcek, Faculty of Chemical Technology, University of Pardubice for the Raman spectra measurements and to Dr. M. Vlcek from Institute of Macromolecular Chemistry of Academy of Sciences of the Czech Republic (present address: Joint Laboratory of Solid State Chemistry of Institute of Macromolecular Chemistry of Academy of Sciences of the Czech Republic and the University of Pardubice) for microprobe X-ray analysis. We acknowledge also to Dipl. Eng. J. Uko for technical assistance.

## References

- [1] A. Nitta, M. Koide, K. Matusita, Eur. J. Glass Sci. Technol. B, **42** (4-5), 275 (2001).
- [2] I. Dyamant, D. Itzhak, J. Hormadaly J. Non-Crystalline Solids **351**, 3503 (2005).
- [3] L.R.P. Kassab, N.D.R. Junior, S.L. Oliveira, J. Non-Cryst. Solids **352**, 3224 (2006).
- [4] S. Bale, M. Purnima, Ch. Srinivasu, S. Rahman J. Alloys Comp. **457**, 545 (2008).
- [5] K. Knoblochova, H. Ticha, J. Schwarz, L. Tichy, Opt.Mater. **31**, 895 (2009).
- [6] Ch. Srinivasu, V. Sathe, A.M. Awasthi, S. Rahman, J. Non-Cryst.Solids **357**, 1051 (2011).
- [7] J. Tauc, Amorphous and Liquid Semiconductors. Plenum Press, New York, 1974.

- [8] J.I. Pankove, *Optical Processes in Semiconductors*. Prentice Hall, Englewood Cliffs, New Jersey, 1971.
- [9] CRC Handbook of Chemistry and Physics 49<sup>th</sup> Edition, 1968-1969, R.C. West (editor), The Chemical Rubby Co., Ohio, USA.
- [10] A.V. Egorysheva, V.I. Burkov, Yu.F. Kargin, V.G. Plotnichenko, V.V. Koltashev, *Crystall.Reports* **50** (1), 135 (2003).
- [11] M.E. Lines, *J. Non-Cryst. Solids* **89**, 141 (1987).
- [12] M.E. Lines, A.E. Miller, K. Nassau and K.B. Lyons, *J. Non-Cryst. Solids* **89**, 163 (1987).
- [13] A.E. Miller, K. Nassau, K.B. Lyons and M.E. Lines, *J. Non.-Cryst. Solids* **99**, 289 (1988).
- [14] G.D. Chryssikos, M.S. Bitsis, J.A. Kapoutsis E.I. Kamitsos, *J. Non-Cryst. Solids* **217**, 278 (1997).
- [15] M. Ganguli, K.J. Rao, *J.Solid State Chem.* **145**, 65 (1999).
- [16] P.J. Bray, *Borate Glass, Structure, Properties, Applications*, ed. I.D. Pye, V.D. Frechette, N. J. Kriedl, Plenum Press, New York (1978).
- [17] P. Zhao, S. Kroeker, J.F. Stebbins, *J. Non.-Cryst. Solids* **276**, 123 (2000).
- [18] F.L. Galeener, J.C. Mikkelsen, R.H. Geils, W.J. Moshby, *Appl.Phys.Lett.* **32**, 34 (1978).
- [19] I.N. Chakraborty, R.A. Condrate Sr., *J. Non-Cryst. Solids* **81**, 271 (1986).
- [20] E.I. Kamitsos, Y.D. Yiannopolous, M.A. Karakassides, G.D. Chryssikos, H. Jain, *J. Phys. Chem.* **100**, 11755 (1996).
- [21] T.S Markova, O.V. Yanush, I.G. Polyakova, B.Z. Pevzner, V.P. Klyuev, *Glass Phys. Chem.* **31**(60) 721 (2005).
- [22] M.B. Volf, *Chemical Approach to Glass*, Elsevier, Amsterdam 1984.
- [23] J.P. Guha, *J. Mat Sci.* **14**, 1744 (1979).
- [24] Y. Takahashi, Y. Benino, T. Fujiwara, T. Komatsu, *J. Non-Cryst. Solids* **316**, 320 (2003).
- [25] P. Pernice, A. Aronne, M. Catauro, A. Marotta, *J. Non-Cryst. Solids* **210**, 23 (1997).
- [26] P.M. Rafailov, A.V. Egorysheva, T.I. Milenov, V.D. Volodin, G.V. Avdeev, R. Titorenkova, V.M. Skorikov, R. Petrova, M.M. Gospodinov, *Appl. Phys. B* **101**, 185 (2010).
- [27] K. Pengpat, D. Holland, *J.Eur.Ceram.Soc.* **23**, 1599 (2003).
- [28] P.S. Yu, L.B. Su, H.L. Tang, X. Guo, H.Y. Zhao, Q.H. Yang, J. Xu, *Sci. China Tech. Sci.* **54**, 1287 (2011).
- [29] S. Polosan, F. Nastace, M. Secu, *J.Non-Cryst. Solids* **357**, 1110 (2011).
- [30] H. Ticha, L. Tichy, P. Nagels, E. Sleafckx, R. Callaerts, *J. Phys. Chem. Sol.* **61**, 545 (2000).
- [31] G.D. Cody Hydrogenated amorphous silicon, Part B: Optical properties, in: J.L. Pankove *Semiconductors and Semimetals 21*, Academic Press, Orlando (1984), p. 11.
- [32] H. Ticha, L. Tichy, *J. Optoelectron. Adv. Mater.* **4**, 381 (2002).

---

\*Corresponding author: Ladislav.Tichy@upce.cz